

# Signal Detection Method Based on Peak to Average Ratio for Frequency Shift Multitone SWIPT System

Takashi Ikeuchi<sup>†</sup>, Yoshihiro Kawahara<sup>†</sup>

<sup>†</sup> Graduate School of Information Science and Technology, The University of Tokyo  
{ikeuchi, kawahara}@aeg.t.u-tokyo.ac.jp

**Abstract**—Battery-less devices that operate on wireless power transfer have a relatively small operating area due to the limited transmit power from the source. Multitone based waveforms are considered to be one of the techniques to expand this operating range. However, they require some bandwidth to achieve this feature. By sharing the bandwidth required for multitone waveforms and superimposing information on the power, it is possible to transmit both power and information at the same time, which is known as simultaneous wireless information and power transfer (SWIPT). In this paper, we introduce a method of detecting signal by measuring peak to average power ratio (PAPR) in order to reduce the computational cost for frequency shift keying type SWIPT instead of observing frequency-domain signals by using fast Fourier transforms. Signal decoding is possible by seeing the PAPR difference as the frequencies of intermodulation signals varies with difference tone arrangement. We demonstrate this through circuit simulation with Advanced Design Systems (ADS) and show how many bits could encode for tones of 3 and 4. In addition, we categories which tone variations in the frequency domain would lead to obtaining a specific PAPR at the receiver end.

**Index Terms**—Energy Harvesting; Frequency Shift Keying; Multitone Based Waveforms; Peak to Average Ratio; Simultaneous Wireless Information and Power Transfer;

## I. INTRODUCTION

Recently, the internet of things (IoT) has been receiving enormous attentions. However, in terms of battery management, embedding batteries in the devices is cumbersome. On the other hand, with the help of recent studies on reducing the energy consumption of sensor devices, some devices operate only by receiving the necessary power from the outer sources. This eliminates the need for recharging or replacing batteries, and hence, more and more sensor devices would be substituted for battery-less or battery-free devices. However, one of the fundamental problems with these devices is that they can only operate in a small area with power from the transmitter because the devices can receive small amount of power. Moreover, as the transmit power is regulated by the government, it is difficult to increase the transmit power.

To overcome this problem, multitone waveforms have gained attention as they generate high peak to average power ratio (PAPR) without increasing the transmitted power by adding several tones. With this feature, diode base rectifiers can yield higher power conversion efficiency (PCE) at the receiving end, thanks to the nonlinearity of diodes [1], [2]. However, one of the drawbacks of multitone waveforms is they consume some bandwidths. If we could transmit power along with signals, we could use signal bandwidth more efficiently.

Simultaneous wireless and information power transfer (SWIPT) is one of a promising approaches to tackle this as it transmits both the power and signal at the same time [3], [4]. There have been extensive works in the wireless communication field, which requires wireless communication modules at the receiving end as well to achieve [3]. Recently, a wireless power transfer (WPT) perspective of SWIPT has been considered. In this scenario, information is superimposed on a power signal, and passive rectifiers are used for acquiring both energy and information [5]–[8].

There are primarily two ways to superimpose information on power; one is to change the number of tones, and the other is to change the size of frequency spacing. In the former case, PAPR differences are considered to know how many tones are added at the transmitter, and in the latter case, fast Fourier transform (FFT) is applied to acquire the variations of frequency spacing [5]–[7], [9]. These methods are beneficial for rectifier based receiver, which does not embed local oscillator or signal front end.

In [5], [9], the trade-offs between the communication rate and the number of tones are revealed. Although increasing the number of tones yields better direct current (DC) output performance, the communication rate deteriorates. In [6], [7], the communication rate is increased, but it is required some additional computational resource when computing FFTs. It is true that a passive filter bank can be used for frequency separation instead of calculating FFTs. However, especially when the communication bandwidth is small, designing a passive filter becomes challenging due to its design requiring a high Q factor. This can also be said about the conventional asynchronous frequency-shift keying (FSK) demodulation. Since we aim to use our technique at an Ultra High Frequency (UHF), communication bandwidth is severely limited. If we could obtain information with a low power measurement method, frequency shift-type SWIPT would become a more realistic approach.

In this paper, we introduce a low power method of demodulation for frequency shift-type SWIPT. Our method utilizes a PAPR based measurement to obtain information instead of directly measuring frequency-domain signals by FFT, which requires high computational cost during the process.

This paper is structured as follows. In Section II, we would introduce the system model of the SWIPT system and show the waveform description of the transmitter and the receiver side. In Section III, we would validate this idea using circuit

simulation for the case of the small number of tones. In Section IV, we would conclude this paper.

## II. SYSTEM MODEL

### A. Signal Description

Multitone based waveforms  $x_T(t)$  at a transmitter can be modeled as follows;

$$x_T(t) = \operatorname{Re} \left\{ \sum_{i=1}^N \sqrt{\frac{P_T}{N}} \exp(j(\omega_i t + \phi_i)) \right\}, \quad (1)$$

where  $N$  represents the number of tones,  $P_T$  is the transmitted power, and  $\omega_i$  is the angular frequency, which is equivalent to  $2\pi f_i$ . Here,  $f_i$  is a carrier frequency of the  $i$ th tone. Let  $\Delta f(i, j)$  be the frequency difference between the  $i$ th tone and  $j$ th tone. We assume  $\Delta f(i, j)$  never goes to negative. Assume the transmit signal has a bandwidth  $BW$ , then the frequency difference between the 1st tone and the  $N$ th tone must satisfy  $\Delta f(1, N) = BW$ . It has been shown that changing the phases of each tone would degrades rectification performance, so we chose the phase to be zero for each tone [10].

At the receiving end, the transmitted signal is received with a channel fading and a noise. We assume here for simplicity that the channel is flat and the noise is negligible as in WPT system, the signal to noise ratio (SNR) is over 30 dB [5]. Now, the received signal  $y_T(t)$  is expressed as follows;

$$y_T(t) = h x_T(t) + n(t). \quad (2)$$

Assuming that the impedance between the antenna and the after the circuit system is matched, the received power at the circuit system does not lose any power. Next, the radio frequency (RF) signal is rectified. During the process of rectification, a diode in the receiver circuit generates harmonic signals, which modulate with each other.

$$\begin{aligned} y_{T_h}(t) &= h \{ C_1 x_T(t) + (C_2 x_T(t))^2 + (C_3 x_T(t))^3 + \dots \} \\ &= C'_1 x_T(t) + (C'_2 x_T(t))^2 + (C'_3 x_T(t))^3 + \dots, \end{aligned} \quad (3)$$

where  $C'_1 = hC_1$ ,  $C'_2 = hC_2$ , and  $C'_3 = hC_3$ . For example, if the 3-tone signal is transmitted, the transmitted and received signal would become following;

$$x_T(t) = \sum_{i=1}^3 a \cos(\omega_i t) \quad (4)$$

$$\begin{aligned} y_{T_h}(t) &= \frac{3}{2} C'_2 a^2 \\ &+ C'_2 a^2 \sum_{i \neq j} \cos(\omega_i t - \omega_j t) \end{aligned} \quad (5)$$

$$\begin{aligned} &+ \left\{ C'_1 a + \frac{15}{4} C'_3 a^3 \right\} \sum_{i=1}^3 \cos(\omega_i t) \\ &+ \frac{3}{4} C'_3 a^3 \left\{ \sum_{i \neq j} \cos(2\omega_i t - \omega_j t) \right\} \\ &+ \frac{3}{2} C'_3 a^3 \left\{ \sum_{i \neq j \neq k, i < j} \cos(\omega_i t + \omega_j t - \omega_k t) \right\} \\ &+ \text{higher order terms,} \end{aligned}$$

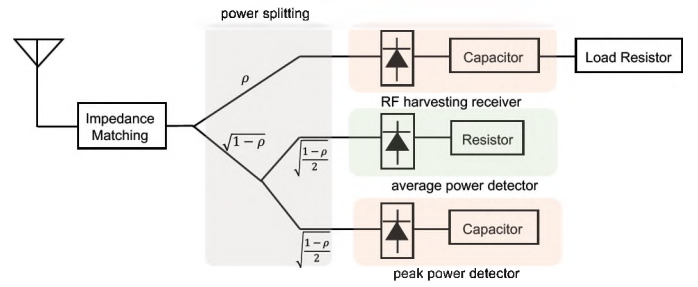


Fig. 1. Block diagram of the SWIPT system. The received signal is split into three paths; one is for the RF harvesting receiver, and the other two modules are placed for calculating the peak voltage, and the average voltage and both of the modules consists of passive elements.

where  $a = \sqrt{\frac{P_T}{N}}$ , and we assume that the signals up to the 3rd order signal would be generated in this case.

### B. Signal Detection

After the rectification, only the differences in frequency spacing can be observed. Changing the frequency spacing results in generating different output PAPR value, so by observing the PAPR differences, it is possible to decode the information that is sent from the transmitter.

For example, when  $N = 3$ , and the frequency differences between the tones are equivalent to one another, i.e.,  $\Delta f(1, 2) = \Delta f(2, 3) = \Delta f$ , the frequency variations of the intermodulation signal have the only  $\Delta f$  except for the higher-order terms. Intermodulation tones would land on the specific points in the frequency domain, which allows the signal powers of these points to accumulate. On the other hand, when the frequency spacings differ from one another, i.e.,  $\Delta f(1, 2) \neq \Delta f(2, 3)$ , the frequency tones that are generated due to the intermodulation would scatter in the frequency domain, deteriorating the signal power. These differences make it possible to differentiate between PAPR values, and therefore, receiver devices can decode information by setting the thresholds according to these differences.

### C. Receiver System Model

A block diagram of a receiver module is shown in Fig. 1. The received signal is split into three paths; one is the main path, which supplies a voltage to the receiver device, and the second path measures the average power, and the third path is for obtaining the peak power. Although in the real case, it is required to calculate the ratio, the modules for obtaining information consist of passive elements. Eliminating compactors or amplifiers leads to suppressing the huge amount of power consumption that would otherwise be required.

## III. SIMULATION VALIDATION

In order to validate this idea, we conducted circuit simulations using an Advanced Design Systems (ADS) to investigate the possibility of distinguishing PAPR with different tone configurations in the frequency domain. We also estimate how many bits would be encodable based on the simulations.

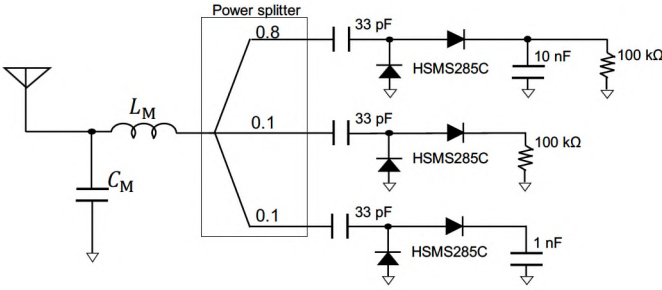


Fig. 2. ADS simulation circuit model. The top path is for the main RF receiver, the next path is a module for getting average power, and the bottom path is a module for obtaining peak power.

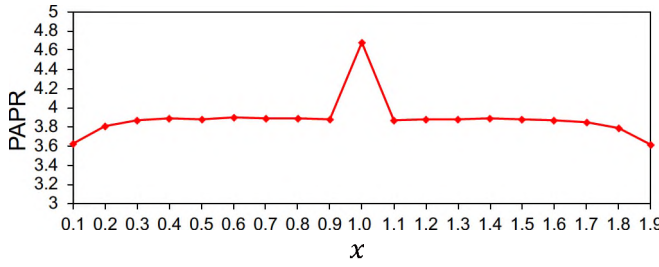


Fig. 3. PAPR comparison between  $\Delta f(1,2) = \Delta f(2,3)$  ( $x = 1.0$ ) and  $\Delta f(1,2) \neq \Delta f(2,3)$  ( $x \neq 1.0$ ) when the received power is  $-10$  dBm.

#### A. PAPR Differences Based on The Tone Placements ( $N = 3$ )

We used Harmonic Balance simulations and calculated the PAPR of the time domain received signals. The number of tones was set to 3, and the bandwidth was fixed to 1 MHz. The generated multitone signals were placed around the 915 MHz carrier frequency. The power allocations of each of the path for obtaining information is 0.1 times smaller than the total received power, respectively. For receiver circuit design, impedance matching was done through the built-in optimization tools in ADS ( $L_M$  and  $C_M$  were optimized in such a way that  $S_{11}$  must be lower than  $-40$  dB) and the diodes we used for rectifications were HSMS295C. We assumed a load resistance of  $100$  k $\Omega$  for the RF harvesting receiver, and a load resistance of  $100$  k $\Omega$  for the path of obtaining average power. For the peak detecting path, we placed a  $1$  nF capacitor. We set three tones to be  $f_c - \frac{BW}{2}$ ,  $f_c - \frac{BW}{2} + x\frac{BW}{2}$ , and  $f_c + \frac{BW}{2}$  respectively, and varied  $x$  from 0.1 to 1.9 to observe the PAPR difference. Here,  $f_c$  is the carrier frequency.

The simulated result when received power ( $P_{in}$ ) is  $-10$  dBm is shown in Fig. 3. The result shows that when  $\Delta f(1,2) = \Delta f(2,3)$ , the PAPR is 4.68, while it is 3.90 at most when  $\Delta f(1,2) \neq \Delta f(2,3)$ . Therefore, based on this result, it is possible to distinguish PAPR differences between  $x = 1.0$ , and  $x \neq 1.0$ . We also found that the third harmonic signals had little effect on the PAPR.

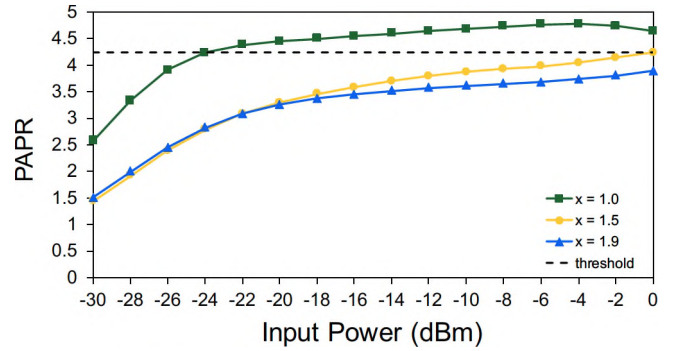


Fig. 4. PAPR comparison between  $\Delta f(1,2) = \Delta f(2,3)$  ( $x = 1.0$ ) and  $\Delta f(1,2) \neq \Delta f(2,3)$  ( $x = 1.5$  and  $x = 1.9$ ) for different received power. Among  $\Delta f(1,2) \neq \Delta f(2,3)$ , we only showed the PAPR that is the highest and lowest, which are  $x = 1.5$  and  $x = 1.9$ , respectively.

TABLE I  
RELATIONSHIP BETWEEN THE NUMBER OF TONES AND THE STATES

Number of tones	2	3	4	5
Number of states	1	2	4	11

#### B. PAPR Differences Based on Received Power ( $N = 3$ )

When the received power varies, the PAPR difference may change, so it is not possible to distinguish what kind of a configuration of the frequency spacing configuration would be sent. Therefore, we tested how the PAPR differences changed when we varied the received power from  $-30$  dBm to  $0$  dBm.

The simulated result is shown in Fig. 4. As can be seen in the figure, the tone configuration of  $x = 1.0$  generated the highest PAPR;  $x = 1.5$  generated the second highest; and  $x = 1.9$  generated the lowest. It was found that when the received power gets smaller, the PAPR for each of the configuration ( $x = 1.0$ ,  $x = 1.5$ ,  $x = 1.9$ ) also becomes smaller. Therefore, it is not possible to distinguish whether  $\Delta f(1,2) = \Delta f(2,3)$  at a low received power or  $\Delta f(1,2) \neq \Delta f(2,3)$  at a high received power. For example, when the input power is  $-30$  dBm, the PAPR for the case of  $\Delta f(1,2) = \Delta f(2,3)$  is 2.58. On the other hand, when the input power is  $0$  dBm, the PAPR for the case of  $\Delta f(1,2) \neq \Delta f(2,3)$  is 4.24. In this case, the receiver does not correctly decode the signal because the value for the case of  $\Delta f(1,2) \neq \Delta f(2,3)$  is higher than that of  $\Delta f(1,2) = \Delta f(2,3)$ . Therefore, a minimum threshold in this case 4.24 is necessary for the receiver to decode correctly. This value is the highest PAPR for the case of  $\Delta f(1,2) \neq \Delta f(2,3)$  (when  $P_{in} = 0$  dBm). After all, the received signal must be above  $-22$  dBm in order to correctly decode the signal in this scheme.

#### C. PAPR Differences For $N = 4$

The previous results showed two states can be obtained with three tones. Therefore, we can send one bit of information. We also found that second-order intermodulation signals have a huge impact on PAPR, while higher-order signals do not influence an effect on it.

TABLE II  
THE CATEGORIES, THE FEATURES OF THE TONES AND THE THRESHOLD PAPR VALUE ( $P_{in} = -10$  dBm)

	tone feature	threshold value	# of variations
Category A	$\Delta f(1,2) = \Delta f(3,4) \wedge \Delta f(1,3) = \Delta f(2,4) \wedge \Delta f(1,2) = \Delta f(2,3)$	5.9	1
Category B	$\Delta f(1,2) = \Delta f(3,4) \wedge \Delta f(1,3) = \Delta f(2,4) \wedge \Delta f(1,2) \neq \Delta f(2,3)$	4.6	13
Category C	$(\Delta f(1,2) = \Delta f(2,3) \wedge \Delta f(1,2) \neq \Delta f(2,3)) \vee (\Delta f(2,3) = f(3,4) \wedge \Delta f(1,2) \neq \Delta f(2,3))$	4.2	54
Category D	Others	3.7	338

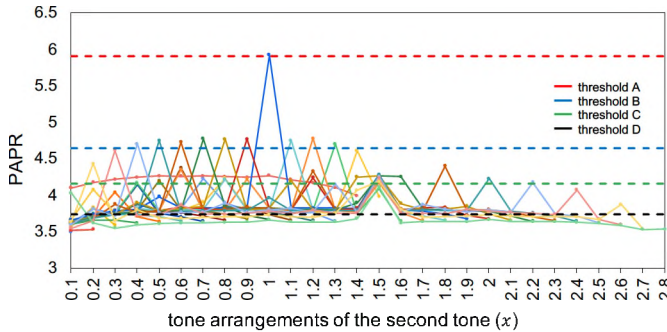


Fig. 5. PAPR comparison when  $N = 4$  and  $-10$  dBm received power.

In order to send more information in a single symbol, it is necessary to increase the number of tones. Since the PAPR variations are based on the second-order intermodulation signals, we can estimate how many bits can be symbolized by counting the number of frequency spacings that have the same value. The result is shown in Tab. I. It is found that increasing the number of tones would lead to increasing the number of PAPR variations.

To validate this, we conducted ADS simulations for the case of 4 tones. The result is shown in Fig. 5. We set the tones to be  $f_c - \frac{BW}{2}$ ,  $f_c - \frac{BW}{2} + x \frac{BW}{3}$ ,  $f_c - \frac{BW}{2} + y \frac{BW}{3}$ , and  $f_c + \frac{BW}{2}$  respectively. We varied  $x$  from 0.1 to  $y$ , and  $y$  from 0.2 to 2.9 to see the PAPR difference. The simulated result is shown in Fig. 5. Based on the result, we could set 4 thresholds. Category A can be grouped around the point where PAPR goes around the threshold A. The only target combination is when  $x = 1.0$ , and  $y = 2.0$ , which means that all the tones in the signal have evenly distributed. In the same way, category B has the frequency spacing with the following feature;  $\Delta f(1,2) = \Delta f(3,4) \wedge \Delta f(1,3) = \Delta f(2,4) \wedge \Delta f(1,2) \neq \Delta f(2,3)$ . The third category has the feature that is when  $(\Delta f(1,2) = \Delta f(2,3) \wedge \Delta f(1,2) \neq \Delta f(3,4)) \vee (\Delta f(2,3) = f(3,4) \wedge \Delta f(1,2) \neq \Delta f(2,3))$ . The other variations of tone arrangements all fall into the category D. The categories, the feature and the threshold value when input power is  $-10$  dBm is listed in Tab. II. This shows that by increasing the number of tones, more bits could be inclusive in a single symbol.

#### IV. CONCLUSIONS

In this paper, a frequency shift-type multitone signal SWIPT system based on PAPR detection method is introduced. The transmitted end varies the frequency spacing of each of the tones in order to encode bits. The receiving end uses multiple

thresholds and decodes based on the received PAPR after the rectification. We validated this idea using the ADS simulations for  $N = 3$  and 4. We also indicated that in order for the receiver side to correctly decode the signal, the minimum received power should be more than  $-22$  dBm for  $N = 3$ .

In the future, we plan on eliminating the power splitter and controlling the current based on load resistances, as it is very difficult to design a power splitter as shown in Fig. 2. Attempting this may cause the PAPR behavior to change or even reverse (when the tones are evenly distributed, then the PAPR becomes the lowest) due to the current flow becoming unstable without a power splitter.

#### ACKNOWLEDGMENT

This work is funded by the JST ERATO Grant Number JPM-JER1501. This work is supported by VLSI Design and Education Center (VDEC), The University of Tokyo with the collaboration with Keysight Technologies

#### REFERENCES

- [1] M. S. Trotter, J. D. Griffin, and G. D. Durgin, "Power-optimized waveforms for improving the range and reliability of rfid systems," in *2009 IEEE International Conference on RFID*, April 2009, pp. 80–87.
- [2] F. Bolos, J. Blanco, A. Collado, and A. Georgiadis, "RF energy harvesting from multi-tone and digitally modulated signals," *IEEE Transactions on Microwave Theory and Techniques*, vol. 64, no. 6, pp. 1918–1927, June 2016.
- [3] T. D. Ponnimbuduge Perera, D. N. K. Jayakody, S. K. Sharma, S. Chatzinotas, and J. Li, "Simultaneous wireless information and power transfer (swipt): Recent advances and future challenges," *IEEE Communications Surveys Tutorials*, vol. 20, no. 1, pp. 264–302, Firstquarter 2018.
- [4] B. Clerckx, "Wireless information and power transfer: Nonlinearity, waveform design, and rate-energy tradeoff," *IEEE Transactions on Signal Processing*, vol. 66, no. 4, pp. 847–862, Feb 2018.
- [5] D. I. Kim, J. H. Moon, and J. J. Park, "New swipt using papr: How it works," *IEEE Wireless Communications Letters*, vol. 5, no. 6, pp. 672–675, Dec 2016.
- [6] M. Rajabi, N. Pan, S. Claessens, S. Pollin, and D. Schreurs, "Modulation techniques for simultaneous wireless information and power transfer with an integrated rectifier-receiver," *IEEE Transactions on Microwave Theory and Techniques*, vol. 66, no. 5, pp. 2373–2385, May 2018.
- [7] S. Claessens, N. Pan, D. Schreurs, and S. Pollin, "Multitone fsk modulation for swipt," *IEEE Transactions on Microwave Theory and Techniques*, vol. 67, no. 5, pp. 1665–1674, May 2019.
- [8] J. Kim, B. Clerckx, and P. D. Mitcheson, "Experimental analysis of harvested energy and throughput trade-off in a realistic swipt system," in *2019 IEEE Wireless Power Transfer Conference (WPTC)*, June 2019, pp. 1–6.
- [9] H. Abbasizadeh, S. Y. Kim, B. Samadpoor Rikan, A. Hejazi, D. Khan, Y. G. Pu, K. C. Hwang, Y. Yang, D. I. Kim, and K.-Y. Lee, "Design of a 900 mhz dual-mode swipt for low-power iot devices," *Sensors*, vol. 19, no. 21, 2019. [Online]. Available: <https://www.mdpi.com/1424-8220/19/21/4676>
- [10] A. S. Boaventura and N. B. Carvalho, "Maximizing dc power in energy harvesting circuits using multisine excitation," in *2011 IEEE MTT-S International Microwave Symposium*, June 2011, pp. 1–4.